



The Impact of Universal Extra Dimensions on FCNC Processes

Andrzej J. Buras^a, Anton Poschenrieder^a, Michael Spranger^{a,b} and Andreas Weiler^a

^a Physik Department, Technische Universität München, D-85748 Garching, Germany

^b Max-Planck-Institut für Physik - Werner-Heisenberg-Institut, D-80805 München, Germany

We review the results of two papers on FCNC processes in the Appelquist, Cheng and Dobrescu (ACD) model with one universal extra dimension.

1 Introduction

Models in more than three spatial dimensions ($D > 4$) have been with us for more than 80 years beginning with the work of Kaluza and Klein, who used this idea in an attempt to unify gravity and electromagnetism in a five dimensional model with the extra compact dimension characterized by a radius R [1].

While Kaluza, Klein and many authors afterwards considered very small extra dimensions with the compactification scale $1/R = \mathcal{O}(M_{\text{Planck}})$, in recent years there has been an increasing interest in models with large extra dimensions, in which $1/R = \mathcal{O}(1 \text{ TeV})$. These models can be classified in particular according to the ability of the fields to live in extra dimensions. In the so-called “brane world” models, the SM fields live only in the usual four dimensions (“SM on the brane”), while gravity lives in the “bulk”, that is in all dimensions [2]. In other models gravity and gauge bosons live in the bulk, while fermions are confined to the brane. In these models $1/R$ has to be larger than a few TeV in order for the model to be consistent with the data. Finally, a special role is played by models with universal extra dimensions (UED) in which all the SM fields are allowed to propagate in all available dimensions. We will concentrate on these models assuming one extra dimension in what follows.

Above the compactification scale $1/R$ a given UED model becomes a higher dimensional field theory whose equivalent description in four dimensions consists of the SM fields, the towers of their Kaluza-Klein (KK) partners and additional towers of KK modes that do not correspond to any field in the SM. Every SM particle has heavy KK partners similar to the case of the MSSM.

The simplest model of this universal type is the Appelquist, Cheng and Dobrescu (ACD) model [3] with one universal extra dimension. In what follows we will briefly describe this model and subsequently report on the results of two papers [4, 5] in which we investigated the impact of the KK modes on FCNC processes in this model.

2 The ACD Model

The full Lagrangian of this model includes both the bulk and the boundary Lagrangian. The bulk Lagrangian is determined by the SM parameters after an appropriate rescaling. The coefficients of the boundary terms, however, although volume suppressed, are free parameters and will get renormalized by bulk interactions. Flavor non-universal boundary terms would lead to large FCNCs. In analogy to a common practice in the MSSM where the soft supersymmetry breaking couplings are chosen to be flavour universal we assume negligible boundary terms at the cut-off scale. With this choice contributions from boundary terms are of higher order and we only have to consider the bulk Lagrangian for the calculation of the impact of the ACD model.

Since all our calculations are cut-off independent (see below) the only additional free parameter relative to the SM is the compactification scale $1/R$.

Thus all the tree-level masses of the KK particles and their interactions among themselves and with the SM particles are described in terms of $1/R$ and the parameters of the SM. This economy in new parameters should be contrasted with supersymmetric theories and models with an extended Higgs sector. All Feynman rules necessary for the evaluation of FCNC processes can be found in [4, 5].

A very important property of the ACD model is the conservation of KK parity that implies the absence of tree level KK contributions to low energy processes taking place at scales $\mu \ll 1/R$. In this context the flavour changing neutral current (FCNC) processes like particle-antiparticle mixing, rare K and B decays and radiative decays are of particular interest. Since these processes first appear at one-loop in the SM and are strongly suppressed, the one-loop contributions from the KK modes to them could in principle be important.

The effects of the KK modes on various processes of interest have been investigated in a number of papers. In [3, 6] their impact on the precision electroweak observables assuming a light Higgs ($m_H \leq 250 \text{ GeV}$) and a

heavy Higgs led to the lower bound $1/R \geq 300\text{GeV}$ and $1/R \geq 250\text{GeV}$, respectively. Subsequent analyses of the anomalous magnetic moment [7] and the $Z \rightarrow b\bar{b}$ vertex [8] have shown the consistency of the ACD model with the data for $1/R \geq 300\text{GeV}$. The latter calculation has been confirmed in [4]. The scale of $1/R$ as low as 300GeV would also lead to an exciting phenomenology in the next generation of colliders and could be of interest in connection with dark matter searches. The relevant references are given in [5].

The question then arises whether such low compactification scales are still consistent with the data on FCNC processes. This question has been addressed in detail in [4, 5]. Before presenting the results of these papers let us recall the particle content of the ACD model that has been described in detail in [4].

In the effective four dimensional theory, in addition to the ordinary particles of the SM, denoted as zero ($n = 0$) modes, there are infinite towers of the KK modes ($n \geq 1$). There is one such tower for each SM boson and two for each SM fermion, while there also exist physical neutral ($a_{(n)}^0$) and charged ($a_{(n)}^\pm$) scalars with ($n \geq 1$) that do not have any zero mode partners. The masses of the KK particles are universally given by

$$(m_{(n)}^2)_{\text{KK}} = m_0^2 + \frac{n^2}{R^2}. \quad (2.1)$$

Here m_0 is the mass of the zero mode, M_W , M_Z , m_t respectively. For $a_{(n)}^0$ and $a_{(n)}^\pm$ this is M_Z and M_W , respectively. In phenomenological applications it is more useful to work with the variables x_t and x_n defined through

$$x_t = \frac{m_t^2}{M_W^2}, \quad x_n = \frac{m_n^2}{M_W^2}, \quad m_n = \frac{n}{R} \quad (2.2)$$

than with the masses in (2.1).

3 The ACD Model and FCNC Processes

As our analysis of [4, 5] shows, the ACD model with one extra dimension has a number of interesting properties from the point of view of FCNC processes discussed here. These are:

- GIM mechanism [9] that improves significantly the convergence of the sum over the KK modes corresponding to the top quark, removing simultaneously to an excellent accuracy the contributions of the KK modes corresponding to lighter quarks and leptons. This feature removes the sensitivity of the calculated branching ratios to the scale $M_s \gg 1/R$ at which the higher dimensional theory becomes non-perturbative and at which the towers of the KK particles must be

cut off in an appropriate way. This should be contrasted with models with fermions localized on the brane, in which the KK parity is not conserved and the sum over the KK modes diverges. In these models the results are sensitive to M_s and for instance in $\Delta M_{s,d}$, the KK effects are significantly larger [10] than found by us. We expect similar behaviour in other processes considered below.

- The low energy effective Hamiltonians are governed by local operators already present in the SM. As flavour violation and CP violation in this model is entirely governed by the CKM matrix, the ACD model belongs to the class of the so-called models with minimal flavour violation (MFV) as defined in [11]. This has automatically the following important consequence for the FCNC processes considered in [4, 5]: the impact of the KK modes on the processes in question amounts only to the modification of the Inami-Lim one-loop functions [12].
- Thus in the case of $\Delta M_{d,s}$ and of the parameter ϵ_K , that are relevant for the standard analysis of the Unitarity Triangle, these modifications have to be made in the function S [13]. In the case of the rare K and B decays that are dominated by Z^0 penguins the functions X and Y [14] receive KK contributions. Finally, in the case of the decays $B \rightarrow X_s \gamma$, $B \rightarrow X_s$ gluon, $B \rightarrow X_s \mu \bar{\mu}$ and $K_L \rightarrow \pi^0 e^+ e^-$ and the CP-violating ratio ϵ'/ϵ the KK contributions to new short distance functions have to be computed. These are the functions D (the γ penguins), E (gluon penguins), D' (γ -magnetic penguins) and E' (chromomagnetic penguins).

Thus each function mentioned above, that in the SM depends only on m_t , becomes now also a function of $1/R$:

$$F(x_t, 1/R) = F_0(x_t) + \sum_{n=1}^{\infty} F_n(x_t, x_n), \quad F = B, C, D, E, D', E', \quad (3.1)$$

with x_n defined in (2.2). The functions $F_0(x_t)$ result from the penguin and box diagrams in the SM and the sum represents the KK contributions to these diagrams.

In the phenomenological applications it is convenient to work with the gauge invariant functions [14]

$$X = C + B^{v\bar{v}}, \quad Y = C + B^{\mu\bar{\mu}}, \quad Z = C + \frac{1}{4}D. \quad (3.2)$$

The functions $F(x_t, 1/R)$ have been calculated in [4, 5] with the results given in table 1. Our results for the function S have been confirmed in [15]. For $1/R = 300\text{ GeV}$, the functions S , X , Y , Z are enhanced by 8%, 10%, 15% and 23% relative to the SM values, respectively. The impact of the KK modes on the function D is negligible. The

function E is moderately enhanced but this enhancement plays only a marginal role in the phenomenological applications. The most interesting are very strong suppressions of D' and E' , that for $1/R = 300 \text{ GeV}$ amount to 36% and 66% relative to the SM values, respectively. However, the effect of the latter suppressions is softened in the relevant branching ratios through sizable additive QCD corrections.

4 The Impact of the KK Modes on Specific Decays

4.1 The Impact on the Unitarity Triangle

Here the function S plays the crucial role. Consequently the impact of the KK modes on the UT is rather small. For $1/R = 300 \text{ GeV}$, $|V_{td}|$, $\bar{\eta}$ and γ are suppressed by 4%, 5% and 5° , respectively. It will be difficult to see these effects in the $(\bar{\rho}, \bar{\eta})$ plane. On the other hand a 4% suppression of $|V_{td}|$ means a 8% suppression of the relevant branching ratio for a rare decay sensitive to $|V_{td}|$ and this effect has to be taken into account. Similar comments apply to $\bar{\eta}$ and γ . Let us also mention that for $1/R = 300 \text{ GeV}$, ΔM_s is enhanced by 8% that in view of the sizable uncertainty in $\hat{B}_{B_s} \sqrt{F_{B_s}}$ will also be difficult to see.

4.2 The Impact on Rare K and B decays

Here the dominant KK effects enter through the function C or equivalently X and Y , depending on the decay considered. In table 2 we show seven branching ratios as functions of $1/R$ for central values of all remaining input parameters. The hierarchy of the enhancements of branching ratios can easily be explained by inspecting the enhancements of the functions X and Y that is partially compensated by the suppression of $|V_{td}|$ in decays sensitive to this CKM matrix element but fully effective in decays governed by $|V_{ts}|$.

For $1/R = 300 \text{ GeV}$ the following enhancements relative to the SM predictions are seen: $K^+ \rightarrow \pi^+ \nu \bar{\nu}$ (9%), $K_L \rightarrow \pi^0 \nu \bar{\nu}$ (10%), $B \rightarrow X_d \nu \bar{\nu}$ (12%), $B \rightarrow X_s \nu \bar{\nu}$ (21%), $K_L \rightarrow \mu \bar{\mu}$ (20%), $B_d \rightarrow \mu \bar{\mu}$ (23%) and $B_s \rightarrow \mu \bar{\mu}$ (33%). These results correspond to central values of the input parameters. The uncertainties in these parameters partly cover the differences between the ACD model and the SM model and it is essential to reduce these uncertainties considerably if one wants to see the effects of the KK modes in the branching ratios in question.

4.3 An Upper Bound on $Br(K^+ \rightarrow \pi^+ \nu \bar{\nu})$ in the ACD Model

The enhancement of $Br(K^+ \rightarrow \pi^+ \nu \bar{\nu})$ in the ACD model is interesting in view of the results from the BNL E787 collaboration at Brookhaven [16] that read

$$Br(K^+ \rightarrow \pi^+ \nu \bar{\nu}) = (15.7^{+17.5}_{-8.2}) \cdot 10^{-11} \quad (4.1)$$

with the central value by a factor of 2 above the SM expectation. Even if the errors are substantial and this result is compatible with the SM, the ACD model with a low compactification scale is closer to the data.

In [17] an upper bound on $Br(K^+ \rightarrow \pi^+ \nu \bar{\nu})$ has been derived within the SM. This bound depends only on $|V_{cb}|$, X , ξ and $\Delta M_d/\Delta M_s$. With the precise value for the angle β now available this bound can be turned into a useful formula for $Br(K^+ \rightarrow \pi^+ \nu \bar{\nu})$ [18] that expresses this branching ratio in terms of theoretically clean observables. In the ACD model this formula reads:

$$Br(K^+ \rightarrow \pi^+ \nu \bar{\nu}) = \bar{\kappa}_+ |V_{cb}|^4 X^2(x_t, 1/R) \times \left[\sigma R_t^2 \sin^2 \beta + \frac{1}{\sigma} \left(R_t \cos \beta + \frac{\lambda^4 P_0(X)}{|V_{cb}|^2 X(x_t, 1/R)} \right)^2 \right], \quad (4.2)$$

where $\sigma = 1/(1 - \lambda^2/2)^2$, $\bar{\kappa}_+ = 7.5 \cdot 10^{-6}$, $P_0(X) \approx 0.40$ and

$$R_t = 0.90 \left[\frac{\xi}{1.24} \right] \sqrt{\frac{18.4/ps}{\Delta M_s}} \sqrt{\frac{\Delta M_d}{0.50/ps}}, \quad \xi = \frac{\sqrt{\hat{B}_{B_s} F_{B_s}}}{\sqrt{\hat{B}_{B_d} F_{B_d}}}. \quad (4.3)$$

This formula is theoretically very clean and does not involve hadronic uncertainties except for ξ and to a lesser extent in $|V_{cb}|$.

In order to find the upper bound on $Br(K^+ \rightarrow \pi^+ \nu \bar{\nu})$ in the ACD model we use $|V_{cb}| \leq 0.0422$, $P_0(X) < 0.47$, $\sin \beta = 0.40$ and $m_t < 172 \text{ GeV}$, where we have set $\sin 2\beta = 0.734$, its central value as $Br(K^+ \rightarrow \pi^+ \nu \bar{\nu})$ depends very weakly on it. The result of this exercise is shown in table 3. We give there $Br(K^+ \rightarrow \pi^+ \nu \bar{\nu})_{\max}$ as a function of ξ and $1/R$ for two different values of ΔM_s . We observe that for $1/R = 250 \text{ GeV}$ and $\xi = 1.30$ the maximal value for $Br(K^+ \rightarrow \pi^+ \nu \bar{\nu})$ in the ACD model is rather close to the central value in (4.1). See [4] for more details.

4.4 The Impact on $B \rightarrow X_s \gamma$ and $B \rightarrow X_s$ gluon

The inclusive $B \rightarrow X_s \gamma$ decay has been the subject of very intensive theoretical and experimental studies during the last 15 years. On the experimental side the world average resulting from the data by CLEO, ALEPH, BaBar and Belle reads [19]

$$Br(B \rightarrow X_s \gamma)_{E_\gamma > 1.6 \text{ GeV}} = (3.28^{+0.41}_{-0.36}) \cdot 10^{-4}. \quad (4.4)$$

It agrees well with the SM result [20, 21]

$$Br(B \rightarrow X_s \gamma)_{E_\gamma > 1.6 \text{ GeV}}^{\text{SM}} = (3.57 \pm 0.30) \cdot 10^{-4}. \quad (4.5)$$

The most recent reviews summarizing the theoretical status can be found in [22, 23, 24].

$1/R$ [GeV]	S	X	Y	Z	E	D'	E'	C	D
200	2.813	1.826	1.281	0.990	0.342	0.113	-0.053	1.099	-0.479
250	2.664	1.731	1.185	0.893	0.327	0.191	0.019	1.003	-0.470
300	2.582	1.674	1.128	0.835	0.315	0.242	0.065	0.946	-0.468
400	2.500	1.613	1.067	0.771	0.298	0.297	0.115	0.885	-0.469
SM	2.398	1.526	0.980	0.679	0.268	0.380	0.191	0.798	-0.476

Table 1. Values for the functions S, X, Y, Z, E, D', E', C and D .

$1/R$	200 GeV	250 GeV	300 GeV	400 GeV	SM
$Br(K^+ \rightarrow \pi^+ \nu \bar{\nu}) \times 10^{11}$	8.70	8.36	8.13	7.88	7.49
$Br(K_L \rightarrow \pi^0 \nu \bar{\nu}) \times 10^{11}$	3.26	3.17	3.09	2.98	2.80
$Br(K_L \rightarrow \mu^+ \mu^-)_{SD} \times 10^9$	1.10	1.00	0.95	0.88	0.79
$Br(B \rightarrow X_s \nu \bar{\nu}) \times 10^5$	5.09	4.56	4.26	3.95	3.53
$Br(B \rightarrow X_d \nu \bar{\nu}) \times 10^6$	1.80	1.70	1.64	1.58	1.47
$Br(B_s \rightarrow \mu^+ \mu^-) \times 10^9$	6.18	5.28	4.78	4.27	3.59
$Br(B_d \rightarrow \mu^+ \mu^-) \times 10^{10}$	1.56	1.41	1.32	1.22	1.07

Table 2. Branching ratios for rare decays in the ACD model and the SM as discussed in the text.

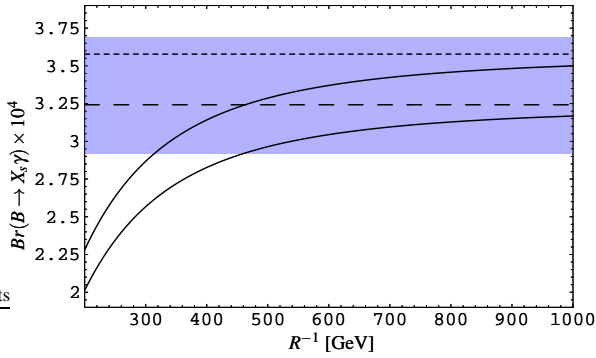


Figure 1. The branching ratio for $B \rightarrow X_s \gamma$ and $E_\gamma > 1.6$ GeV as a function of $1/R$. See text for the meaning of various curves.

Due to strong suppressions of the functions D' and E' by the KK modes, the $B \rightarrow X_s \gamma$ and $B \rightarrow X_s$ gluon decays are considerably suppressed compared to SM estimates. For $1/R = 300$ GeV, $Br(B \rightarrow X_s \gamma)$ is suppressed by 20%, while $Br(B \rightarrow X_s \text{ gluon})$ even by 40%. The phenomenological relevance of the latter suppression is unclear at present as $Br(B \rightarrow X_s \text{ gluon})$ suffers from large theoretical uncertainties and its extraction from experiment is very difficult if not impossible.

In fig. 1 we compare $Br(B \rightarrow X_s \gamma)$ in the ACD model with the experimental data and with the expectations of the SM. The shaded region represents the data in (4.4) and the upper (lower) dashed horizontal line are the central values in the SM for $m_c/m_b = 0.22$ ($m_c/m_b = 0.29$). The solid lines represent the corresponding central values in the ACD model. The theoretical errors, not shown in the plot, are for all

curves roughly $\pm 10\%$

We observe that in view of the sizable experimental error and considerable parametric uncertainties in the theoretical prediction, the strong suppression of $Br(B \rightarrow X_s \gamma)$ by the KK modes does not yet provide a powerful lower bound on $1/R$ and the values $1/R \geq 250$ GeV are fully consistent with the experimental result. It should also be emphasized that $Br(B \rightarrow X_s \gamma)$ depends sensitively on the ratio m_c/m_b and the lower bound on $1/R$ is shifted above 400 GeV for $m_c/m_b = 0.29$ if other uncertainties are neglected. In order to reduce the dependence on m_c/m_b a NNLO calculation is required. Once it is completed and the experimental uncertainties reduced, $Br(B \rightarrow X_s \gamma)$ may provide a very powerful bound on $1/R$ that is substantially stronger than the bounds obtained from the electroweak precision data.

The suppression of $Br(B \rightarrow X_s \gamma)$ in the ACD model has already been found in [25]. Our result presented above is consistent with the one obtained by these authors but differs in details as only the dominant diagrams have been taken into account in the latter paper and the analysis was performed in the LO approximation.

4.5 The Impact on $B \rightarrow X_s \mu^+ \mu^-$ and $A_{FB}(\hat{s})$

The inclusive $B \rightarrow X_s \mu^+ \mu^-$ decay has been the subject of very intensive theoretical and experimental studies during the last 15 years. On the experimental side only the BELLE collaboration reported the observation of this decay with [26]

$$Br(B \rightarrow X_s \mu^+ \mu^-) = (7.9 \pm 2.1_{-1.5}^{+2.0}) \cdot 10^{-6}. \quad (4.6)$$

For the decay to be dominated by perturbative contributions one has to remove $\bar{c}c$ resonances by appropriate kin-

ξ	$1/R = 200 \text{ GeV}$	$1/R = 250 \text{ GeV}$	$1/R = 300 \text{ GeV}$	$1/R = 400 \text{ GeV}$	SM
1.30	13.8* (12.3*)	12.7* (11.3*)	12.0* (10.7)	11.3* (10.1)	10.8 (9.3)
1.25	13.0* (11.6)	12.0 (10.7)	11.4 (10.2)	10.7 (9.6)	10.3 (8.8)
1.20	12.2* (10.9)	11.3 (10.1)	10.7 (9.6)	10.1 (9.1)	9.7 (8.4)
1.15	11.5 (10.3)	10.6 (9.5)	10.1 (9.0)	9.5 (8.5)	9.1 (7.9)

Table 3. Upper bound on $Br(K^+ \rightarrow \pi^+ \nu \bar{\nu})$ in units of 10^{-11} for different values of ξ , $1/R$ and $\Delta M_s = 18/\text{ps}$ (21/ps). The stars indicate the results corresponding to $\sqrt{\hat{B}_{B_d} F_{B_d}} \leq 190 \text{ MeV}$.

matic cuts in the dilepton mass spectrum. The SM expectation [27] for the low dilepton mass window is given by

$$\tilde{B}r(B \rightarrow X_s \mu^+ \mu^-)_{\text{SM}} = (2.75 \pm 0.45) \cdot 10^{-6} \quad (4.7)$$

where the dilepton mass spectrum has been integrated between the limits:

$$\left(\frac{2m_\mu}{m_b}\right)^2 \leq \hat{s} \leq \left(\frac{M_{J/\psi} - 0.35 \text{ GeV}}{m_b}\right)^2 \quad (4.8)$$

where $\hat{s} = (p_+ + p_-)^2 / m_b^2$.

This cannot be directly compared to the experimental result in (4.6) that is supposed to include the contributions from the full dilepton mass spectrum. Fortunately future experimental analyses should give the results corresponding to the low dilepton mass window so that a direct comparison between the experiment and the theory will be possible. The most recent reviews summarizing the theoretical status can be found in [24, 27].

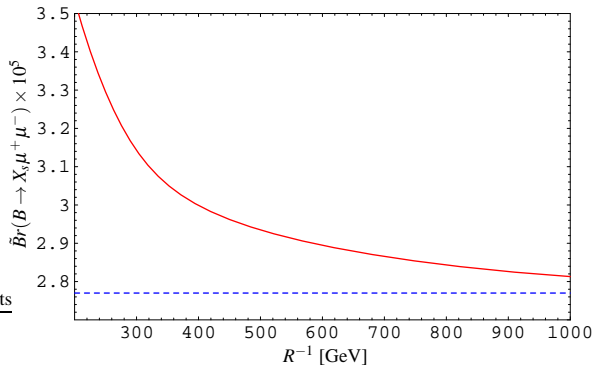


Figure 2. $\tilde{B}r(B \rightarrow X_s \mu^+ \mu^-)$ in the SM (dashed line) and in the ACD model. The integration limits are discussed in the text.

In fig. 2 we show the branching ratio $\tilde{B}r(B \rightarrow X_s \mu^+ \mu^-)$ as a function of $1/R$ that corresponds to the SM result of (4.7). The observed enhancement is mainly due to the function Y that enters the Wilson coefficient of the operator $(\bar{s}b)_{V-A}(\bar{\mu}\mu)_A$. The Wilson coefficient of $(\bar{s}b)_{V-A}(\bar{\mu}\mu)_V$, traditionally denoted by C_9 , is essentially unaffected by the KK contributions.

Of particular interest is the Forward-Backward asymmetry $A_{\text{FB}}(\hat{s})$ in $B \rightarrow X_s \mu^+ \mu^-$ that similarly to the case of exclusive decays [28] vanishes at a particular value $\hat{s} = \hat{s}_0$. The fact that $A_{\text{FB}}(\hat{s})$ and the value of \hat{s}_0 being sensitive to short distance physics are in addition subject to only very small non-perturbative uncertainties makes them particularly useful quantities to test physics beyond the SM.

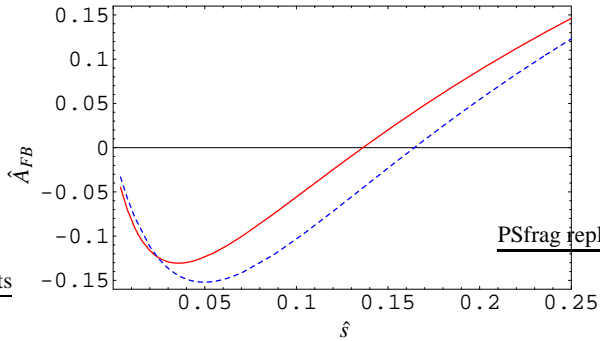
The calculations for $A_{\text{FB}}(\hat{s})$ and of \hat{s}_0 have recently been done including NNLO corrections [29, 30] that turn out to be significant. In particular they shift the NLO value of \hat{s}_0 from 0.142 to 0.162 at NNLO. In fig. 3 (a) we show the normalized Forward-Backward asymmetry that we obtained by means of the formulae and the computer program of [27, 29] modified by the KK contributions calculated in [5]. The dependence of \hat{s}_0 on $1/R$ is shown in fig. 3 (b).

We observe that the value of \hat{s}_0 is considerably reduced relative to the SM result obtained by including NNLO corrections [27, 29, 30]. This decrease is related to the decrease of $Br(B \rightarrow X_s \gamma)$ as discussed below. For $1/R = 300 \text{ GeV}$ we find the value for \hat{s}_0 that is very close to the NLO prediction of the SM. This result demonstrates very clearly the importance of the calculations of the higher order QCD corrections, in particular in quantities like \hat{s}_0 that are theoretically clean. We expect that the results in figs. 3 (a) and (b) will play an important role in the tests of the ACD model in the future.

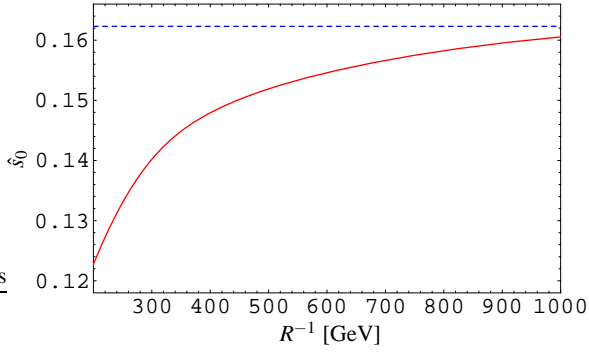
In MFV models there exist a number of correlations between different measurable quantities that do not depend on specific parameters of a given model [11, 31]. In [5] a correlation between \hat{s}_0 and $Br(B \rightarrow X_s \gamma)$ has been pointed out. It is present in the ACD model and in a large class of supersymmetric models discussed for instance in [27]. We show this correlation in fig. 4. We refer to [5] for further details.

4.6 The Impact on $K_L \rightarrow \pi^0 e^+ e^-$ and ϵ'/ϵ

The impact of the KK modes on the rare decay $K_L \rightarrow \pi^0 e^+ e^-$ is at most 10% but it is substantially larger on ϵ'/ϵ . The most recent discussion on ϵ'/ϵ can be found in [32]. As the Z^0 penguins are enhanced in the ACD model, the ratio ϵ'/ϵ is suppressed relative to the SM expectations with the size of the suppression depending sensitively on



(a)



(b)

Figure 3. (a) Normalized Forward-Backward asymmetry in the SM (dashed line) and ACD for $R^{-1} = 250$ GeV. (b) Zero of the forward backward asymmetry A_{FB} in the SM (dashed line) and the ACD model.

the hadronic matrix elements. In view of this no useful bound on $1/R$ can be obtained from ε'/ε at present.

5 Concluding Remarks

Our analysis of the ACD model shows that all the present data on FCNC processes are consistent with $1/R$ as low as 250 GeV, implying that the KK particles could in principle be found already at the Tevatron. Possibly, the most interesting results of our analysis is the enhancement of $Br(K^+ \rightarrow \pi^+ \nu \bar{\nu})$, the sizable downward shift of the zero ($\hat{\delta}_0$) in the A_{FB} asymmetry and the suppression of $Br(B \rightarrow X_s \gamma)$.

The nice feature of this extension of the SM is the presence of only one additional parameter, the compactification scale. This feature allows a unique determination of various enhancements and suppressions relative to the SM expectations. We find

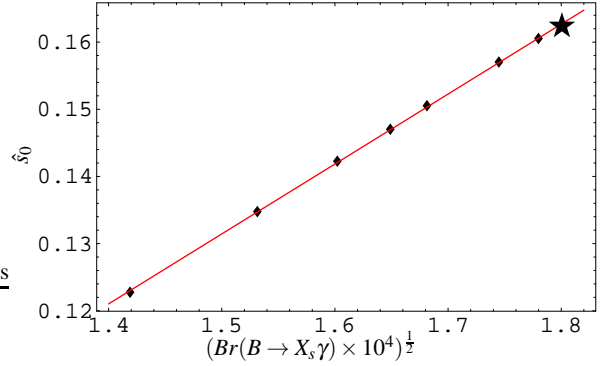


Figure 4. Correlation between $\sqrt{Br(B \rightarrow X_s \gamma)}$ and $\hat{\delta}_0$. The straight line is a least square fit to a linear function. The dots are the results in the ACD model for $1/R = 200, 250, 300, 350, 400, 600$ and 1000 GeV and the star denotes the SM value.

- Enhancements: $K_L \rightarrow \pi^0 e^+ e^-$, ΔM_s , $K^+ \rightarrow \pi^+ \nu \bar{\nu}$, $K_L \rightarrow \pi^0 \nu \bar{\nu}$, $B \rightarrow X_d \nu \bar{\nu}$, $B \rightarrow X_s \nu \bar{\nu}$, $K_L \rightarrow \mu^+ \mu^-$, $B_d \rightarrow \mu^+ \mu^-$, $B \rightarrow X_s \mu^+ \mu^-$ and $B_s \rightarrow \mu^+ \mu^-$.
- Suppressions: $B \rightarrow X_s \gamma$, $B \rightarrow X_s$ gluon, the value of $\hat{\delta}_0$ in the forward-backward asymmetry and ε'/ε .

We would like to emphasize that violation of this pattern by the future data will exclude the ACD model. For instance the measurement of $\hat{\delta}_0$ that is higher than the SM estimate would automatically exclude this model as there is no compactification scale for which this could be satisfied. Whether these enhancements and suppressions are required by the data or whether they exclude the ACD model with a low compactification scale, will depend on the precision of the forthcoming experiments and the efforts to decrease the theoretical uncertainties.

Acknowledgements

This research was partially supported by the German ‘Bundesministerium für Bildung und Forschung’ under contract 05HT1WOA3 and by the ‘Deutsche Forschungsgemeinschaft’ (DFG) under contract Bu.706/1-2.

References

1. T. Kaluza, Sitzungsber. Preuss. Akad. Wiss. Berlin (Math. Phys.) **1921** (1921) 966; O. Klein, Z. Phys. **37** (1926) 895 [Surveys High Energ. Phys. **5** (1986) 241].
2. I. Antoniadis, N. Arkani-Hamed, S. Dimopoulos and G. R. Dvali, Phys. Lett. B **436** (1998) 257 [arXiv:hep-ph/9804398].
3. T. Appelquist, H. C. Cheng and B. A. Dobrescu, Phys. Rev. D **64** (2001) 035002 [arXiv:hep-ph/0012100].
4. A. J. Buras, M. Spranger and A. Weiler, Nucl. Phys. B **660** (2003) 225 [arXiv:hep-ph/0212143].

5. A. J. Buras, A. Poschenrieder, M. Spranger and A. Weiler, arXiv:hep-ph/0306158.
6. T. Appelquist and H. U. Yee, Phys. Rev. D **67** (2003) 055002 [arXiv:hep-ph/0211023].
7. K. Agashe, N. G. Deshpande and G. H. Wu, Phys. Lett. B **511** (2001) 85 [arXiv:hep-ph/0103235].
8. J. F. Oliver, J. Papavassiliou and A. Santamaria, Phys. Rev. D **67** (2003) 056002 [arXiv:hep-ph/0212391].
9. S. L. Glashow, J. Iliopoulos and L. Maiani, Phys. Rev. D **2** (1970) 1285.
10. J. Papavassiliou and A. Santamaria, Phys. Rev. D **63** (2001) 016002 [arXiv:hep-ph/0008151]; J. F. Oliver, J. Papavassiliou and A. Santamaria, arXiv:hep-ph/0209021.
11. A. J. Buras, P. Gambino, M. Gorbahn, S. Jager and L. Silvestrini, Phys. Lett. B **500** (2001) 161 [arXiv:hep-ph/0007085].
12. T. Inami and C. S. Lim, Prog. Theor. Phys. **65** (1981) 297 [Erratum-ibid. **65** (1981) 1772].
13. A. J. Buras, W. Slominski and H. Steger, Nucl. Phys. B **238** (1984) 529; Nucl. Phys. B **245** (1984) 369.
14. G. Buchalla, A. J. Buras and M. K. Harlander, Nucl. Phys. B **349** (1991) 1.
15. D. Chakraverty, K. Huitu and A. Kundu, Phys. Lett. B **558** (2003) 173 [arXiv:hep-ph/0212047].
16. S. C. Adler *et al.* [E787 Collaboration], Phys. Rev. Lett. **79** (1997) 2204 [arXiv:hep-ex/9708031]; Phys. Rev. Lett. **84** (2000) 3768 [arXiv:hep-ex/0002015]; Phys. Rev. Lett. **88** (2002) 041803 [arXiv:hep-ex/0111091].
17. G. Buchalla and A. J. Buras, Nucl. Phys. B **548** (1999) 309 [arXiv:hep-ph/9901288].
18. G. D'Ambrosio and G. Isidori, Phys. Lett. B **530** (2002) 108 [arXiv:hep-ph/0112135].
19. M. Battaglia *et al.*, arXiv:hep-ph/0304132.
20. P. Gambino and M. Misiak, Nucl. Phys. B **611** (2001) 338 [arXiv:hep-ph/0104034].
21. A. J. Buras, A. Czarnecki, M. Misiak and J. Urban, Nucl. Phys. B **631** (2002) 219 [arXiv:hep-ph/0203135].
22. A. J. Buras and M. Misiak, Acta Phys. Polon. B **33** (2002) 2597 [arXiv:hep-ph/0207131].
23. A. Ali and M. Misiak in [19].
24. T. Hurth, arXiv:hep-ph/0212304.
25. K. Agashe, N. G. Deshpande and G. H. Wu, Phys. Lett. B **514** (2001) 309 [arXiv:hep-ph/0105084].
26. J. Kaneko *et al.* [Belle Collaboration], Phys. Rev. Lett. **90** (2003) 021801 [arXiv:hep-ex/0208029].
27. A. Ali, E. Lunghi, C. Greub and G. Hiller, Phys. Rev. D **66** (2002) 034002 [arXiv:hep-ph/0112300].
28. G. Burdman, Phys. Rev. D **57** (1998) 4254 [arXiv:hep-ph/9710550].
29. H. H. Asatrian, H. M. Asatrian, C. Greub and M. Walker, Phys. Lett. B **507** (2001) 162 [arXiv:hep-ph/0103087]; Phys. Rev. D **65** (2002) 074004 [arXiv:hep-ph/0109140]; Phys. Rev. D **66** (2002) 034009 [arXiv:hep-ph/0204341]; H. M. Asatrian, K. Bieri, C. Greub and A. Hovhannisyian, Phys. Rev. D **66** (2002) 094013 [arXiv:hep-ph/0209006].
30. A. Ghinculov, T. Hurth, G. Isidori and Y. P. Yao, Nucl. Phys. B **648** (2003) 254 [arXiv:hep-ph/0208088]; arXiv:hep-ph/0211197.
31. A. J. Buras and R. Fleischer, Phys. Rev. D **64** (2001) 115010 [arXiv:hep-ph/0104238]; A. J. Buras and R. Buras, Phys. Lett. B **501** (2001) 223 [arXiv:hep-ph/0008273]; S. Bergmann and G. Perez, JHEP **0008** (2000) 034 [arXiv:hep-ph/0007170]; Phys. Rev. D **64** (2001) 115009 [arXiv:hep-ph/0103299]; S. Laplace, Z. Ligeti, Y. Nir and G. Perez, Phys. Rev. D **65** (2002) 094040 [arXiv:hep-ph/0202010]; A. J. Buras, arXiv:hep-ph/0303060.
32. A. J. Buras and M. Jamin, arXiv:hep-ph/0306217.